Published OnlineFirst September 28, 2017; DOI: 10.1158/2326-6066.CIR-16-0303

seeded as coculture in 200 μL DMEM with 5% heat-inactivated FBS in cell-repellent surface 96-well microplates (Greiner Bio-One) and immediately centrifuged at 180 × *g* for 1 minute. Spheroid formation was observed after overnight incubation.

Immune cell quantification in the spheroids

Immune cells were added to the spheroids 3 days after seeding. Peripheral blood mononuclear cells (PBMCs) were isolated from buffy coats from healthy donors by Ficoll centrifugation and immediately frozen. Thawed PBMCs were filtered and pan-T cells and NK cells were isolated using MACS (Miltenyi Biotec). One hour after addition of a serial dilution of NOX-A12, 5×10^4 immune cells were added per well for overnight incubation. Spheroids were washed three times with PBS to remove loosely attached immune cells. Spheroids were dissociated using Accumax (eBiosciences) for 90 minutes for immune cell quantification by flow cytometry (Guava easyCyte, Millipore).

Immunohistochemistry (IHC)

Spheroids were washed with PBS three times and fixed with 10% (v/v) neutral buffered formalin for 2 hours. After paraffinization, 2-μm slides were cut for H&E or immunostaining. The following antibodies were used: panCK (DAKO, #M0821), CXCL12 (R&D Systems, #MAB350), CD3 (DAKO, #A0452). IHC experiments were performed by Provitro GmbH (Germany). T cells were counted by three blinded observers.

3D PD-1–dependent T-cell activation reporter assay

In order to investigate T-cell activation in the spheroids, a PD-1/PD-L1 blockade reporter bioassay (Promega) was adapted to the 3D format that used an alternative readout from traditional primary cell-based assays. Primary T cells were replaced with a Jurkat cell line stably expressing TCR, PD-1, and NFAT-inducible luciferase. The target cells were CHO-K1 cells expressing human PD-L1 and an engineered cell surface protein designed to activate cognate TCRs in an antigen-independent manner. When cocultured, TCR activation of the Jurkat cells induced the NFAT pathway, whereas PD-1 signaling decreased it. Upon addition of an anti–PD-1 or anti–PD-L1 agent, the Jurkat–TCR axis induced NFAT-mediated luciferase expression that can be detected by addition of Bio-Glo reagent and quantified with a luminometer. Briefly, Jurkat$^{\text{PD-1/luc}}$T cells (5×10^4/well) were preincubated with anti–PD-1 (clone PD1.3.1.3, Miltenyi Biotec) for 30 minutes and subsequently added to tumor–stroma spheroids (CHO$^{\text{PD-L1}}$ + MS-5; $0.5 \times 10^4 + 2.5 \times 10^4$/well, respectively) in the presence or absence of NOX-A12. The next day, T-cell infiltration was quantified by flow cytometry as described above. T-cell activation was quantified after incubating the spheroids in 75 μL medium (DMEM + 5% FBS) with 50 μL BioGlo substrate (Promega) for 45 minutes. Relative luminescence of anti–PD-1 and/or NOX-A12–treated spheroids was normalized to untreated spheroids. Combination Index was calculated using CompuSyn software (ComboSyn, Inc.).

CT-26 *in vivo* efficacy study

Female BALB/c mice (6–7 weeks, Shanghai Lingchang Biotechnology Co. Ltd) were subcutaneously inoculated with 5×10^5 CT-26 colon cancer cells (Shanghai Institutes for Biological Sciences) at the right lower flank. Tumor growth was monitored three times per week by caliper measurement. Tumor volume was calculated using the formula: $V = 0.5\ a \times b^2$ where a and b are the long and short diameters of the tumor, respectively. NOX-A12 (20 mg/kg s.c., every other day) treatment was initiated at day 5 when mean tumor volume (MTV) reached approximately 50 mm^3. Anti–PD-1 (RMP1-14, BioXCell, 10 mg/kg i.p., twice weekly) treatment was initiated at day 7 when MTV in untreated mice reached approximately 100 mm^3. Mice were sacrificed at day 20. All *in vivo* experiments were performed at Crown Bioscience Inc. in accordance with the regulations of the Association for Assessment and Accreditation of Laboratory Animal Care.

Statistical analysis

Differences of infiltrated T cells between groups in IHC were quantified by the Student *t* test. In FACS analysis of spheroids two-way ANOVA was used with the Dunnet test for multiple comparisons to compare NOX-A12–treated spheroids to nontreated ones. Tumor volumes were analyzed using a global Kruskal–Wallis test. In case of a statistically significant effect, this was followed by pairwise Wilcoxon rank sum tests (SPSS, version 18.0, IBM; and SAS 9.4, SAS Institute Inc.). All tests were two-sided. $P < 0.05$ was considered statistically significant. Statistical analyses were performed by SCO:SSiS Consulting.

Results

For mechanistic *in vitro* studies on the role of CXCL12 in lymphocyte tumor infiltration, heterotypic 3D spheroids consisting of CXCL12-secreting MS-5 stromal cells and the pancreatic cancer cell line PSN-1 were established. We found that NOX-A12 enhanced the infiltration of primary human T cells into PSN-1/MS-5 spheroids in a dose-dependent manner. The number of NK cells in the spheroids was also enhanced by CXCL12 inhibition. Likewise, B cells infiltrated the microtissue but to a lesser extent. Infiltration of monocytes was not observed (Fig. 1A). A closer look into the T-cell subsets by using isolated primary pan-T cells revealed a similar infiltration rate for CD8$^+$ and CD4$^+$ T cells, whereas Tregs migrated to a lesser degree into the spheroids after treatment with NOX-A12 (Fig. 1B). IHC analysis of paraffin-embedded sections showed a homogeneous distribution of tumor cells (PanCK staining) and stromal cells throughout the spheroids (Fig. 1C). CXCL12 was evenly expressed in the spheroid apart from the necrotic core which resembles a real tumor. IHC staining confirmed the finding of enhanced T-cell infiltration in the presence of NOX-A12 in the PSN-1/MS-5 spheroids as well as in the HT-29/MS-5 spheroids. The crescent-formed CD3$^+$ T-cell localization of the latter spheroids was likely due to the fact that only the bottom of the spheroid had contact with the T cells and the cultures were not shaken overnight (Fig. 1D).

Next, we confirmed the enhanced lymphocyte infiltration upon CXCL12 inhibition in various other spheroid types using MS-5 stromal cells and tumor cell lines from four different origins (PSN-1 pancreatic adenocarcinoma cells, HT-29 colorectal carcinoma cells, H1299 non–small cell lung cancer cells, and U251MG glioblastoma cells). In addition to T cells, the effect of CXCL12 inhibition on the migration of primary NK cells was tested in these experiments. We found a similar dose-dependent increase in spheroid T-cell infiltration in all four spheroid types. Approximately 30% of the T cells that were added to the assay infiltrated the spheroids at baseline. The addition of 10 nmol/L NOX-A12 led to a 2- to 3-fold increase in spheroid T-cell infiltration

Published OnlineFirst September 28, 2017; DOI: 10.1158/2326-6066.CIR-16-0303

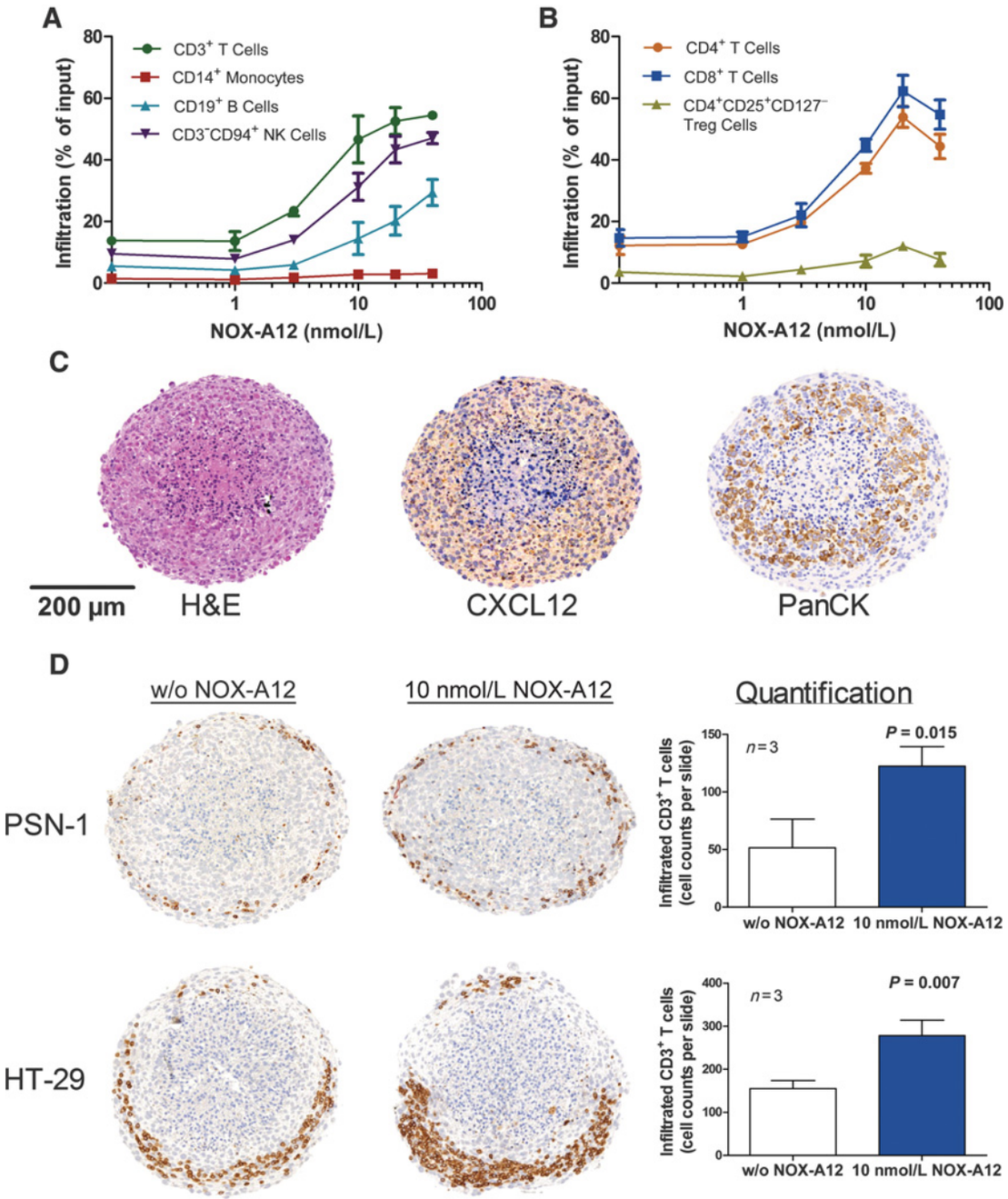

Figure 1.

Effect of NOX-A12 treatment on immune-cell infiltration into tumor–stroma spheroids. Spheroids consisting of CXCL12-expressing MS-5 stromal cells and PSN-1 pancreatic adenocarcinoma cells were generated. Peripheral blood mononuclear cells (**A**) or isolated primary human pan T cells (**B–D**) were added to the spheroids in the presence of various concentrations of NOX-A12. The next day, immune cell infiltration was quantified by flow cytometry (**A**, **B**). Alternatively, spheroids were paraffin-embedded for H&E or immunostaining (**C**, **D**). The tumor cell marker PanCK (pan-cytokeratin) revealed a homogeneous distribution of stromal and tumor cells in the spheroid which colocalized with the presence of CXCL12 (**C**). NOX-A12 increased the amount of $CD3^+$ T cells (brown spots) in both tumor–stroma spheroid models (PSN-1 and HT-29). Bar graphs indicate the numbers of $CD3^+$ T cells (mean ± SD) in sections of three different spheroids per group, counted by three individual analysts (**D**). Data are representative of three or more independent experiments.

(Fig. 2A). The baseline of NK-cell infiltration was lower (5%–10%). However, when NOX-A12 was added to the spheroids, the NK-cell infiltration rate increased up to 8-fold (Fig. 2B).

To analyze whether enhanced T-cell infiltration would boost the efficacy of checkpoint inhibition, we used a bioluminescent PD-1/PD-L1 blockade reporter bioassay that we have adapted to

Published OnlineFirst September 28, 2017; DOI: 10.1158/2326-6066.CIR-16-0303

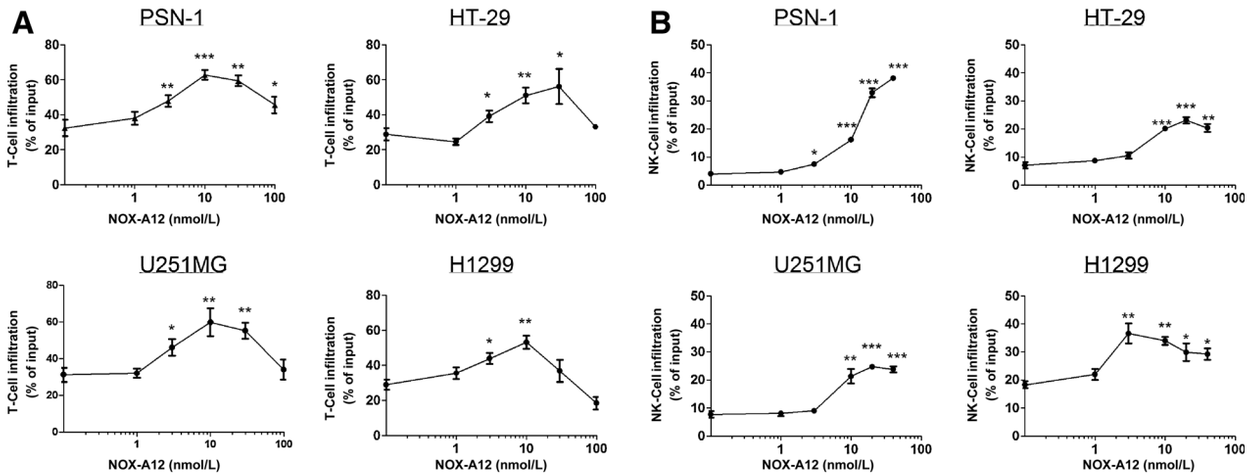

Figure 2.

NOX-A12 increases NK- and T-cell infiltration in various tumor–stroma spheroid models. Spheroids composed of MS-5 stromal cells and various cancer cell lines (PSN-1 pancreatic ductal adenocarcinoma, HT-29 colorectal carcinoma, H1299 non–small cell lung cancer, and U251MG glioblastoma) were treated with various concentrations of NOX-A12 and exposed to isolated primary human T cells (**A**) or NK cells (**B**) from healthy donors. After incubation overnight, infiltrated lymphocytes were quantified by flow cytometry. Results indicate immune cell infiltration relative to input cell counts representing the mean ± SD values of triplicates. Data are representative of three or more independent experiments. *, $P < 0.05$; **, $P < 0.01$; ***, $P < 0.001$.

the 3D format by generating spheroids consisting of MS-5 stromal cells with the CHO$^{PD\text{-}L1}$ cancer cell line. Jurkat$^{PD\text{-}1/luc}$ T cells were incubated with these spheroids in the presence or absence of NOX-A12. As expected, we found increased T-cell infiltration after CXCL12 inhibition by 10 nmol/L NOX-A12, whereas anti–PD-1 treatment did not influence T-cell trafficking (Fig. 3A). Macroscopically, enhanced T-cell migration into the spheroids was suggested by a reduced number of surrounding T cells (Fig. 3B). NOX-A12 treatment alone dose-dependently increased Jurkat T-cell activation, whereas the effect of treatment with anti–PD-

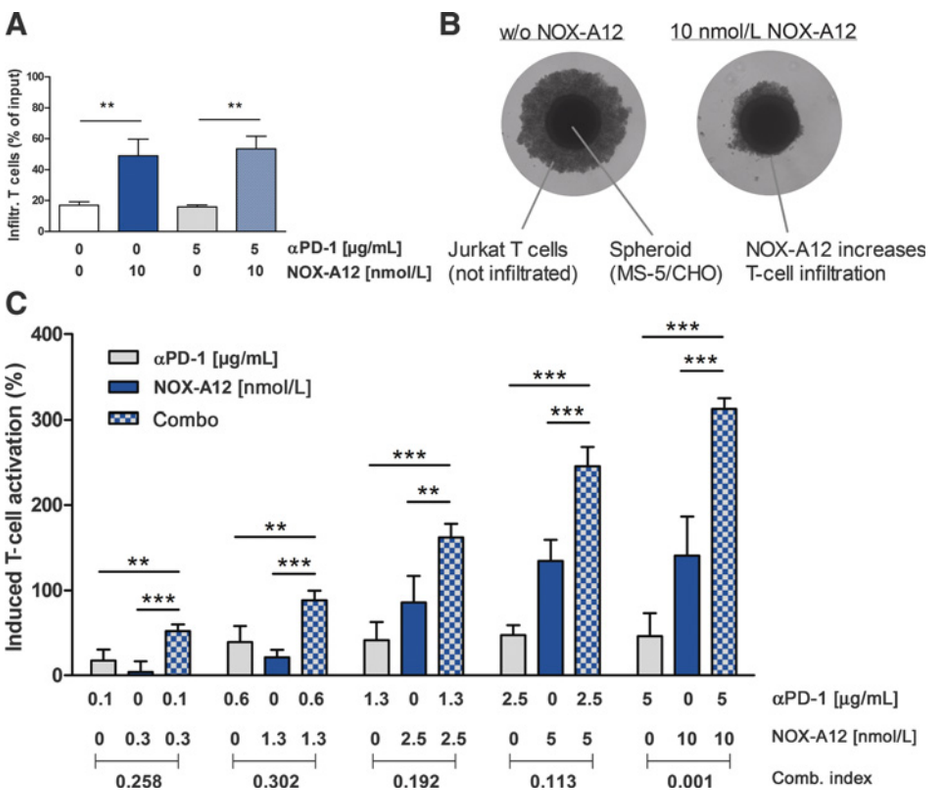

Figure 3.

NOX-A12 synergizes with PD-1 checkpoint inhibition *in vitro*. A reporter-based PD-1/PD-L1 blockade bioassay was adapted to the 3D format: Spheroids consisting of MS-5 stromal cells and CHO$^{PD\text{-}L1}$ cancer cells were incubated with NOX-A12 and exposed to Jurkat$^{PD\text{-}1/luc}$ T cells in the presence or absence of anti–PD-1 antibody. The next day, T-cell infiltration was quantified by flow cytometry (**A**) and visualized by light microscopy (**B**). T-cell activation was quantified by incubating the spheroids with BioGlo substrate (**C**). T-cell activation (relative luminescence) was normalized to untreated spheroids. The mean ± SD values of triplicates are shown. Data are representative of three independent experiments. Combination index below 1 indicating synergy was calculated using CompuSyn software. *, $P < 0.05$; **, $P < 0.01$; ***, $P < 0.001$.

Published OnlineFirst September 28, 2017; DOI: 10.1158/2326-6066.CIR-16-0303

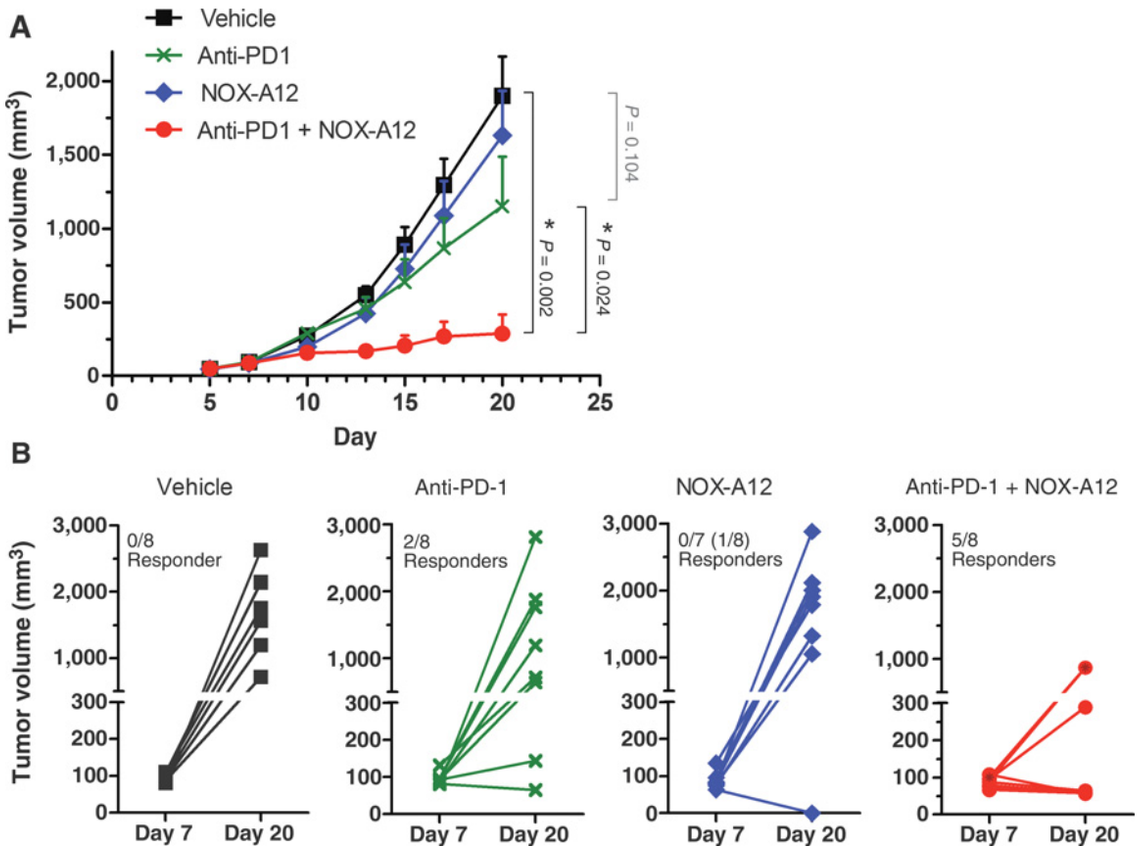

Figure 4.

NOX-A12 synergizes with PD-1 checkpoint inhibition *in vivo*. Mice were subcutaneously inoculated with CT-26 colon cancer cells. Treatment with NOX-A12 (20 mg/kg s.c., every other day) and anti–PD-1 (10 mg/kg i.p. twice weekly) was initiated at days 5 and 7, respectively. **A,** Mean tumor volumes (± SEM, $n = 8$ per group) of mice treated with vehicle (black squares), anti–PD-1 (green crosses), NOX-A12 (blue diamonds), or anti–PD-1/NOX-A12 combination (red circles). *, $P < 0.05$. **B,** Tumor volumes of individual mice prior to anti–PD-1 treatment (day 7) and at the end of experiment (day 20). Mice with stable or reduced tumor volumes below 200 mm^3 were considered as responders. The experiment was repeated at another independent contract research organization *(Oncodesign, Dijon, FR)* with similar results.

1 alone was rather weak. This is likely due to the fact that most of the T cells were located outside the anti–PD-1-treated spheroid whereas NOX-A12 facilitated the physical contact between effector and target. Consequently, the combination of anti–PD-1 with NOX-A12 synergistically increased T-cell activation (Fig. 3C), with a combination index of 0.001 (14).

The *in vivo* efficacy of NOX-A12/anti–PD-1 combination treatment was assessed in the murine syngeneic CT-26 colon cancer model. Mice treated with anti–PD-1 alone showed a nonsignificant reduction in tumor growth by day 20 ($P = 0.104$) with only 2 out of 8 mice responding (Fig. 4A and B). NOX-A12 monotherapy did not significantly reduce tumor growth ($P = 0.564$ vs. vehicle). However, when NOX-A12 treatment was combined with anti–PD-1 treatment, efficacy was enhanced with significantly reduced tumor volumes compared with either vehicle ($P = 0.002$) or anti–PD-1 monotherapy ($P = 0.024$). In fact, in this group, 5 of 8 mice responded to the treatment (Fig. 4A and B). The experiment was repeated at another independent contract research organization (Oncodesign) with similar results. This result confirms the potential of CXCL12-inhibition to enhance the efficacy of anti–PD-1 treatment.

Discussion

The success of immune checkpoint inhibitors in a subset of cancer patients has raised interest in combining these therapies with other agents to broaden their applicability (4, 15). Checkpoint inhibitors are only able to unleash antitumor T-cell responses in an immunogenic TME. Therefore, turning an immunosuppressive tumor into an immunogenic tumor is necessary for successful cancer immunotherapy (2). Several combination therapies have been proposed that combine checkpoint inhibitors with other checkpoint inhibitors, inhibitors of suppressive metabolites, vaccines, targeted therapies, cytotoxics, and/or radiotherapy (16). Manipulation of T-cell trafficking into the tumor has rarely been addressed (3). Here, we provide evidence for the use of the CXCL12 inhibitor NOX-A12 to improve checkpoint inhibitor efficacy by enhancing T- and NK-cell migration into the tumor.

We used tumor–stroma spheroids in order to assess immune-cell infiltration. This approach allows a quantitative assessment of immune cell trafficking by flow cytometry. A similar spheroid model was used previously to evaluate NK-cell infiltration (17); however, we included CXCL12-expressing stromal cells in our

Published OnlineFirst September 28, 2017; DOI: 10.1158/2326-6066.CIR-16-0303

tumor spheroids to investigate the role of this chemokine in immune cell trafficking. We assessed immune cell infiltration by all main components of PBMCs and observed that CXCL12 inhibition enhanced infiltration of $CD8^+$ T cells, $CD4^+$ T cells, and NK cells, and to a lesser extent Treg and B cells into the tumor–stroma spheroids. We found that NOX-A12, which facilitates physical contact of T cells with their targets by inhibiting CXCL12, complements checkpoint inhibition and thus synergized with anti–PD-1 in the spheroid model.

The synergy of anti–PD-1 with NOX-A12 was corroborated *in vivo*, thus validating our spheroid approach. The CT-26 model was chosen because it contains cancer-associated fibroblasts which contribute to tumor growth (18) and is not controlled by anti–PD-1 treatment. The improved efficacy of anti–PD-1 therapy when delivered in combination with NOX-A12 is comparable with the results reported for combined PD-1 and CTLA-4 checkpoint inhibition in this model (19). The combined checkpoint inhibitor approach has been translated into the clinic, but is associated with increased toxicity (20). A combination of NOX-A12 with checkpoint inhibitors may thus improve cancer immunotherapy (21) due to both its mode of action and the good safety profile seen so far for other NOX-A12 combinations in clinical trials (12, 13).

NOX-A12 dose dependently increased immune cell infiltration up to a point. At very high NOX-A12 concentrations, fewer lymphocytes were observed in the spheroids. Of note, NOX-A12 did not alter the spheroid composition of cell types, as we have not observed any toxicity or viability decrease of tumor, stroma, or immune cells in the presence of high NOX-A12 concentrations *in vitro*. The eventual decrease of immune cell infiltration could thus be explained by the nonlinear effects of CXCL12, which attracts T cells at low to intermediate concentrations but repels them at high concentrations (22–24). We therefore hypothesize that by partially neutralizing CXCL12 in the outer areas, NOX-A12 generates a CXCL12 gradient within the spheroid which immune cells can follow, whereas at high NOX-A12 concentrations, all CXCL12 is blocked and therefore less migration occurs. The generation of CXCL12 gradients that lead into the dense tumor structure differentiates agents that directly target CXCL12 from CXCR4 antagonists that may enhance T-cell infiltration particularly in cases of high local CXCL12 concentrations (6, 25). On the contrary, the generation of chemotactic gradients by CXCL12-neutralizing agents may enhance T-cell infiltration into tumors for which the CXCL12 expression level is low enough to attract T cells but too homogeneous to give a directional clue to the lymphocytes. Clinical development of NOX-A12 as an inhibitor of CXCL12 is running concurrently with clinical development of various antagonists of the receptor CXCR4.

In conclusion, we have shown *in vitro* and in an animal model that inhibition of CXCL12 by NOX-A12 can help to overcome the resistance to anti–PD-1 treatment. We anticipate that this concept can also be extended to inhibition of other checkpoints such as CTLA-4, TIM-3, and LAG-3, because NOX-A12 appears to break through the immune-privileged status of the TME, thereby paving the way for T-cell migration into the tumor. Considering NOX-A12 enhanced infiltration by not only T cells but also NK cells, which mediate antibody-dependent cellular cytotoxicity, a combination therapy that includes antibodies targeting immune checkpoints on cancer cells (e.g., PD-L1) seems reasonable. Furthermore, NOX-A12 has the potential to increase the efficacy of a variety of immuno-oncology approaches, including tumor vaccines, bispecific T-cell–engaging antibodies or modified immune cells, such as CAR-T and CAR-NK cells or TCR-modified T cells. A phase I/II clinical trial is currently ongoing to study the effects of combining NOX-A12 and anti–PD-1 treatment in patients with late-line colorectal cancer and pancreatic ductal adenocarcinoma (NCT03168139).

Disclosure of Potential Conflicts of Interest

D. Eulberg is VP Project Management at NOXXON Pharma AG. A. Vater has ownership interest (including patents) in NOXXON Pharma AG. No potential conflicts of interest were disclosed by the other authors.

Authors' Contributions

Conception and design: D. Zboralski, K. Hoehlig, D. Eulberg, A. Frömming, A. Vater
Development of methodology: D. Zboralski
Acquisition of data (provided animals, acquired and managed patients, provided facilities, etc.): D. Zboralski
Analysis and interpretation of data (e.g., statistical analysis, biostatistics, computational analysis): D. Zboralski, K. Hoehlig, A. Frömming
Writing, review, and/or revision of the manuscript: D. Zboralski, K. Hoehlig, D. Eulberg, A. Frömming, A. Vater
Other (interpretation of data in terms of hypothesis generation): A. Vater

Acknowledgments

The authors would like to thank Lisa Bauer and Sophie Barsin for assistance in 3D cell culture, Provitro AG for IHC services, Crown Bioscience and Oncodesign for performing the CT-26 mouse experiments, and SCO:SSiS Consulting for help with statistical analysis.

Received November 1, 2016; revised July 14, 2017; accepted September 22, 2017; published OnlineFirst September 28, 2017.

References

1. Fridman WH, Pagès F, Sautès-Fridman C, Galon J. The immune contexture in human tumours: impact on clinical outcome. Nat Rev Cancer 2012; 12:298–306.
2. Melero I, Rouzaut A, Motz GT, Coukos G. T-cell and NK-cell infiltration into solid tumors: a key limiting factor for efficacious cancer immunotherapy. Cancer Discov 2014;4:522–6.
3. Joyce JA, Fearon DT. T cell exclusion, immune privilege, and the tumor microenvironment. Science 2015;348:74–80.
4. Sharma P, Allison JP. The future of immune checkpoint therapy. Science 2015;348:56–61.
5. Guo F, Wang Y, Liu J, Mok SC, Xue F, Zhang W. CXCL12/CXCR4: a symbiotic bridge linking cancer cells and their stromal neighbors in oncogenic communication networks. Oncogene 2016;35:816–26.
6. Feig C, Jones JO, Kraman M, Wells RJ, Deonarine A, Chan DS, et al. Targeting CXCL12 from FAP-expressing carcinoma-associated fibroblasts synergizes with anti–PD-L1 immunotherapy in pancreatic cancer. Proc Natl Acad Sci U S A 2013;110:20212–7.
7. Fearon DT. The carcinoma-associated fibroblast expressing fibroblast activation protein and escape from immune surveillance. Cancer Immunol Res 2014;2:187–93.
8. Vater A, Klussmann S. Turning mirror-image oligonucleotides into drugs: the evolution of Spiegelmer therapeutics. Drug Discov Today 2015; 20:147–55.
9. Roccaro AM, Sacco A, Purschke WG, Moschetta M, Buchner K, Maasch C, et al. SDF-1 inhibition targets the bone marrow niche for cancer therapy. Cell Rep 2014;9:118–28.

Published OnlineFirst September 28, 2017; DOI: 10.1158/2326-6066.CIR-16-0303

10. Hoellenriegel J, Zboralski D, Maasch C, Rosin NY, Wierda WG, Keating MJ, et al. The Spiegelmer NOX-A12, a novel CXCL12 inhibitor, interferes with chronic lymphocytic leukemia cell motility and causes chemosensitization. Blood 2014;123:1032–9.
11. Liu SC, Alomran R, Chernikova SB, Lartey F, Stafford J, Jang T, et al. Blockade of SDF-1 after irradiation inhibits tumor recurrences of autochthonous brain tumors in rats. Neuro-oncology 2014;16:21–8.
12. Ludwig H, Weisel K, Petrucci MT, Leleu X, Cafro AM, Garderet L, et al. Olaptesed pegol, an anti-CXCL12/SDF-1 Spiegelmer, alone and with bortezomib-dexamethasone in relapsed/refractory multiple myeloma: a phase IIa study. Leukemia 2017;31:997–1000.
13. Steurer M, Montillo M, Scarfò L, Mauro FR, Andel J, Wildner S, et al. Results from a phase IIa study of the anti-CXCL12 spiegelmer olaptesed pegol (NOX-A12) in combination with bendamustine/rituximab in patients with chronic lymphocytic leukemia. Blood 2014;124:1996.
14. Chou TC. Drug combination studies and their synergy quantification using the Chou–Talalay method. Cancer Res 2010;70:440–6.
15. Mahoney KM, Rennert PD, Freeman GJ. Combination cancer immunotherapy and new immunomodulatory targets. Nat Rev Drug Discov 2015; 14:561–84.
16. Melero I, Berman DM, Aznar MA, Korman AJ, Pérez Gracia JL, Haanen J. Evolving synergistic combinations of targeted immunotherapies to combat cancer. Nat Rev Cancer 2015;15:457–72.
17. Giannattasio A, Weil S, Kloess S, Ansari N, Stelzer EH, Cerwenka A, et al. Cytotoxicity and infiltration of human NK cells in in vivo-like tumor spheroids. BMC Cancer 2015;15:351.
18. Santos AM, Jung J, Aziz N, Kissil JL, Puré E. Targeting fibroblast activation protein inhibits tumor stromagenesis and growth in mice. J Clin Invest 2009;119:3613–25.
19. Duraiswamy J, Kaluza KM, Freeman GJ, Coukos G. Dual blockade of PD-1 and CTLA-4 combined with tumor vaccine effectively restores T-cell rejection function in tumors. Cancer Res 2013;73:3591–603.
20. Callahan MK, Postow MA, Wolchok JD. CTLA-4 and PD-1 pathway blockade: combinations in the clinic. Front Oncol 2014;4:385.
21. Mellman I, Hubbard-Lucey VM, Tontonoz MJ, Kalos MD, Chen DS, Allison JP, et al. De-risking immunotherapy: report of a consensus workshop of the Cancer Immunotherapy Consortium of the Cancer Research Institute. Cancer Immunol Res 2016;4:279–88.
22. Boneschansker L, Yan J, Wong E, Briscoe DM, Irimia D. Microfluidic platform for the quantitative analysis of leukocyte migration signatures. Nat Commun 2014;5:4787.
23. Dunussi-Joannopoulos K, Zuberek K, Runyon K, Hawley RG, Wong A, Erickson J, et al. Efficacious immunomodulatory activity of the chemokine stromal cell-derived factor 1 (SDF-1): local secretion of SDF-1 at the tumor site serves as T-cell chemoattractant and mediates T-cell-dependent antitumor responses. Blood 2002;100:1551–8.
24. Poznansky MC, Olszak IT, Foxall R, Evans RH, Luster AD, Scadden DT. Active movement of T cells away from a chemokine. Nat Med 2000;6:543–8.
25. Chen Y, Ramjiawan RR, Reiberger T, Ng MR, Hato T, Huang Y, et al. CXCR4 inhibition in tumor microenvironment facilitates anti-programmed death receptor-1 immunotherapy in sorafenib-treated hepatocellular carcinoma in mice. Hepatology 2015;61:1591–602.

Published OnlineFirst September 28, 2017; DOI: 10.1158/2326-6066.CIR-16-0303

Cancer Immunology Research

Increasing Tumor-Infiltrating T Cells through Inhibition of CXCL12 with NOX-A12 Synergizes with PD-1 Blockade

Dirk Zboralski, Kai Hoehlig, Dirk Eulberg, et al.

Cancer Immunol Res 2017;5:950-956. Published OnlineFirst September 28, 2017.